AN ANOMALY IN INTERCEPT TIME FOR SHORT RANGE BALLISTIC RE-ENTRY VEHICLES

P. Bao U. Nguyen

Maude Amyot-Bourgeois
Brittany C. Astles

Defence Research Development Canada
Centre for Operational Research and Analysis
National Defence Headquarters (Carling)
60 Moodie Drive
Ottawa, ON K2H 8G1, CANADA
and
Department of Mathematics and Statistics
University of Ottawa
STEM Complex, room 336
150 Louis-Pasteur Pvt
Ottawa, ON K1N 6N5, CANADA

Defence Research Development Canada
Centre for Operational Research and Analysis
National Defence Headquarters (Carling)
60 Moodie Drive
Ottawa, ON K2H 8G1, CANADA

ABSTRACT

This paper documents an anomaly in intercept time of a ballistic re-entry vehicle (RV) by a ballistic interceptor. Intuitively, it is expected that as soon as an incoming RV is detected, the defense will launch an interceptor. However, we show that under some conditions (short range, lofted RV trajectory and an interceptor that is slower than the RV) it is best to delay the launch of the interceptor so that the intercept time is minimal. This is important since by minimizing the intercept time, the interceptor can intercept the RV earlier, further away from the defense location and therefore safer for the defense. In addition, with minimal intercept times, the defense may maximize the number of engagement opportunities. This will allow the defense to improve the probability of raid negation. That is, the probability of neutralizing all incoming RVs is greater with more engagement opportunities. We will show how to minimize the intercept time using analysis in the phase space (velocities of the RV and the interceptor) and validate the results using MANA (Map-Aware Non-uniform Automata).

1   INTRODUCTION

Generally, ballistic vehicle trajectories can be determined using astrodynamics (Bate et al. 1971; Vallado 1997). Intermediate and long range ballistic missile defense is described for example by (Buontempo 2015; Carnegie Endowment for International Peace 2021; Weitz 2013). We consider the problem of short range ballistic missile defense.

In this context, the earth is flat with gravitational acceleration equal to $g = 9.81 \ m/sec^2$. The trajectory of a ballistic vehicle is completely determined by the initial conditions i.e. the initial location and the initial velocity of the vehicle. To intercept an RV, the interceptor detonates when it reaches a non-zero weapon range to the RV.

The intercept equations are simple when the weapon range is zero. However, the intercept time solution becomes complex when the weapon range is non-zero. That is, the problem becomes intractable using calculus as it would involve a sixth order polynomial with hundreds of terms once the derivative is radicalized (Nguyen and Nguyen 1996).

We derive an analytical solution to the intercept time using geometry in the velocity phase space (Nguyen et al. 2022). This solution includes many parameters: the RV initial location, the RV initial velocity, the interceptor initial location, the interceptor launch delay time, the interceptor speed, the detonation range and gravity.

With this solution, we obtain the intercept time as a function of the interceptor launch delay time. To our surprise, it is not always better to launch the interceptor as soon as the RV is detected in the sense that to minimize the intercept time, sometimes it is best to delay the launch of the interceptor. We refer to this phenomenon as the anomaly in intercept time for short range ballistic RVs. If the intercept time is minimized, the defense may maximize the number of engagement opportunities and thereby maximize the probability of raid negation (the probability of neutralizing all incoming RVs). Therefore, the number of engagement opportunities is a key metric as described in (Armstrong 2014; Bourn 2012; Nguyen 2014; Soland 1987; Nguyen et al. 1997; Wilkening 1999; Mury and Nguyen 2007; Menq et al. 2007; Cranford).

This paper is organized as follows. Section 2 provides examples based on realistic data showing the anomaly. Section 3 describes briefly the derivation of intercept time. Section 4 presents an algorithm to minimize the intercept time based on the interceptor launch delay time. We conclude in Section 5.

2 EXAMPLES

For illustrations, we assume that the RV has similar capabilities as those of the Scud missiles deployed during the gulf war by Iraq in 1990 – 1991 and the interceptor has similar capabilities as those of the Patriot missiles. Their characteristics are shown below (Patriot 2022).

Table 1: Characteristics of the RV where MACH 1 is the speed of sound 0.343 km/s .

Scud Type	Speed (*km/s*)	Range (*km*) and Location (*Range, 0,0*)
Scud A		180
Scud B	1.7 (MACH 5)	300
Scud C		600
Scud D		700

Table 2: Characteristics of the interceptor.

Speed	MACH 2, 3, 4
Range (*km*)	50, 100, 150, 200
Detonation Range (*m*)	1, 2, 5

The defense (target of the RV) and the interceptor launch site are co-located at the origin for the simplicity of the illustration. We also assume that the RV is launched from the maximal ranges of the interceptor. Figure 1 shows the trajectories of the RV for multiple ranges: $50 \, km$ to $200 \, km$ away from the defense location. The RV assumes an initial speed equal to $MACH$ 5. There are two types of trajectories: the dashed lines correspond to the low angle trajectories while the solid lines correspond to the high angle trajectories. We refer the low angle (high angle) trajectories as the depressed (lofted) trajectories. The depressed trajectories have a maximal $z \leq 20 \, km$ and the lofted trajectories have a maximal $z \geq 120 \, km$ where z is the altitude of the RV. Here, the RV is launched from the ground ($z = 0$), travels from right to left, and aims for the defense location at the origin $(0,0)$.

Figure 2 shows the time it takes to intercept the RV as a function of the interceptor launch delay time for multiple ranges, where intercept time is from RV launch to RV intercept. The interceptor assumes a speed equal to $MACH$ 4.
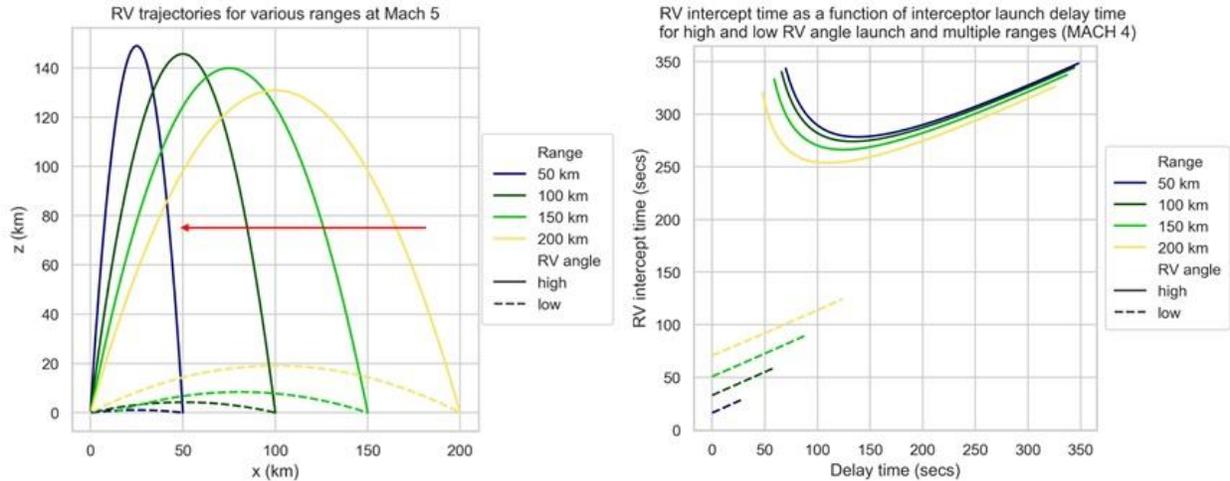

Figure 1: RV lofted (high) and depressed (low) trajectories.

Figure 2: The RV intercept time as a function of the interceptor launch delay time for multiple ranges with interceptor speed equal to MACH 4 for lofted (high) and depressed (low) RV trajectories.

The intercept times for the depressed trajectories are less than $125\ secs$ (dashed lines) and those for the lofted trajectories are more than $250\ secs$ (solid lines). The intercept times increase with the interceptor delay time for the depressed trajectories. However, the intercept times decrease and then increase with the interceptor delay time for the lofted trajectories. We analyze the intercept time of the lofted trajectory with a range of $200\ km$ (solid yellow curve) shown in Figure 2 above. In *Case 1*, if the defense waited for $50\ secs$ after the RV is launched from a $200\ km$ range at a lofted trajectory, the intercept occurs at approximately $300\ secs$. In *Case 2,* if the defense waited for $100\ secs$ after the RV is launched from a $200\ km$ range at a lofted trajectory, the intercept occurs at approximately $250\ secs$. This includes the $100\ secs$ delay. That is, the RV is launched at time zero, the interceptor is launched at time $100\ secs$ and the intercept occurs at time $250\ secs$. This means that the time of flight of the interceptor is $150\ secs$ ($250 - 100 = 150\ secs$). At this interceptor launch delay time, we note that the RV intercept time is also a minimum. With an interceptor launch delay time equal to $50\ secs$ ($100\ secs$) the RV intercept time is equal to $300\ secs$ ($250\ secs$). The time line for Case 1 and Case 2 are shown in Figure 3.
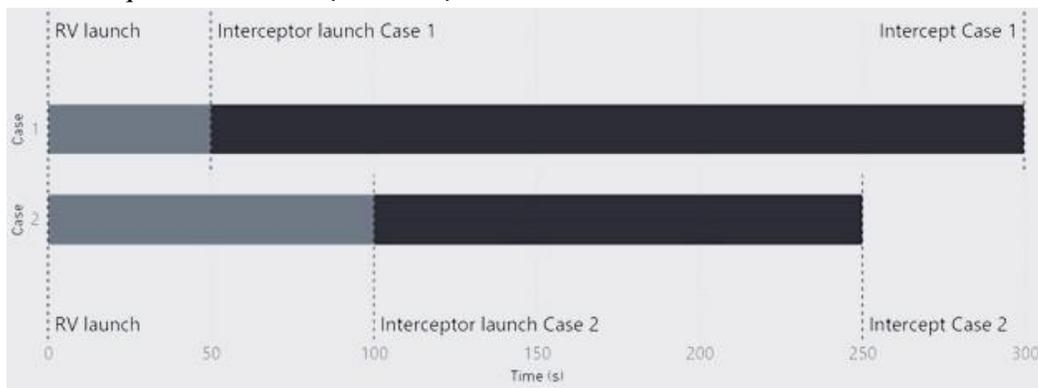

Figure 3: An example of intercept time line.

To validate our results, we make use of MANA (Map-Aware Non-uniform Automata) which is an agent-based model developed by the Defence Technology Agency of New Zealand (Lauren and Stephen 2003). Agent-based simulations and characteristics are described by (Castle and Crooks 2006) and (Diallo et al. 2016). MANA was used by (Amyot-Bourgeois et al. 2021a) and (Serré et al. 2021) for data farming and by (Amyot-Bourgeois et al. 2021b) for a ground-based air defense scenario. The comparisons between our results (dash line) and those from MANA (bold line) are consistent as shown in Figure 4. Even though we only show the comparisons for the lofted trajectories, those for the depressed trajectories were also made and validated.

Intuitively, it is expected that the earlier the interceptor is launched, the sooner the RV is intercepted. Clearly, this is not the case as with the shorter launch delay of 50 $secs$ (compared to 100 $secs$), the RV intercept time occurs at a later time of 300 $secs$ (compared to 250 $secs$). We refer to this phenomenon as the anomaly in intercept time that occurs for lofted trajectories based on numerical results. We examine this anomaly in the following sections.

3   FORMULA FOR THE INTERCEPT TIME

Nguyen, Amyot-Bourgeois and Astles derive the intercept time formula for an interceptor exploding at a non–zero detonation range from the RV. t_{int} is the earliest intercept time in the sense it is the shortest time for the interceptor to reach the detonation range from the RV given an interceptor launch delay time t measured from the launch time of the RV. Therefore, t_{int} is a function of t. Among the possible interceptor launch delay time t, there could be a minimal intercept time , t_{int} as shown in Figure 4. The formula for t_{int} is needed for examining such a trend.

$$t_{\text{int}} = \frac{\Delta r^0}{v} \cdot \left(\frac{-F + \sqrt{F^2 + \left(1 - \beta^2\right) \cdot \left(1 - \alpha^2\right)}}{1 - \beta^2} \right) \tag{1}$$

where F , $\alpha,$ β and $cos(\theta^0)$ are dimensionless and are defined as:

$$F = \alpha + \beta \cdot \cos\left(\theta^0\right), \quad \beta = \frac{u}{v}, \quad \alpha = \frac{\alpha_0}{\Delta r^0} \quad \text{and} \quad \cos\left(\theta^0\right) = \frac{\vec{u} \cdot \vec{\Delta r}^0}{u \cdot \Delta r^0} .$$

$\left(x_i^0, y_i^0, z_i^0\right)$ is the position of the launch site of the interceptor; $\left(x_m^0, y_m^0, z_m^0\right)$ is the position of the RV at the interceptor launch time (this is not necessarily the position of the launch site of the RV as the defense might delay the launch of the interceptor while the RV is travelling); $\Delta \vec{r}^0 = \left(x_m^0 - x_i^0, y_m^0 - y_i^0, z_m^0 - z_i^0\right)$; α_0 is the detonation range; $\vec{u}(t) = \vec{u} - g \cdot t \cdot \hat{z}$ is the velocity of the RV subjected to gravity and it is known while v is the speed of the interceptor. We note that Equation (1) is not trivial since the argument of the square root is a sixth order polynomial in time t for a non – zero detonation range. The RV intercept time accounting for the interceptor launch delay time is equal to T=$t + t_{int}(t)$. This is shown for example on the vertical axis of Figures 2 and 4. Using the intercept time in Equation (1), we can also determine the direction of the velocity of the interceptor (Nguyen, Amyot-Bourgeois and Astles *forthcoming*). There are two steps in determining the trajectory of the interceptor due to the particularity of the solution. First, we generate a straight line solution. Second, we add gravity to the straight line solution.

Figure 5 shows the intercept of the RV trajectories in orange and the interceptor trajectories in blue without gravity. The RV moves from right to left while the interceptor moves from left to right. The solid lines correspond to the lofted trajectories while the dashed lines correspond to the depressed trajectories. The RV is intercepted when the trajectories intersect one another. These are the straight line solutions.
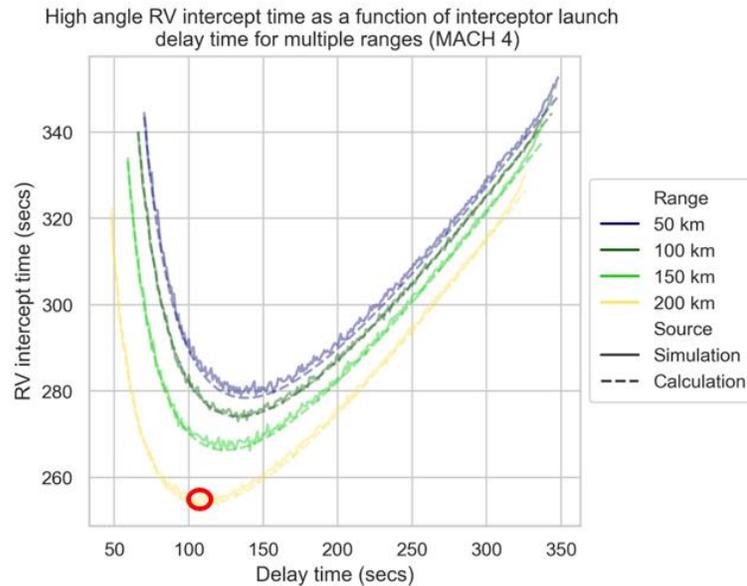
Figure 4: RV (lofted trajectories) intercept time as a function of interceptor launch delay time for multiple ranges obtained from MANA (bold line) and calculation (dash line) (interceptor speed MACH 4).

Figure 6 shows the physical intercept of the RV trajectories in orange and the interceptor trajectories in blue with gravity. The RV moves from right to left and the interceptor moves from left to right. The solid lines correspond to the lofted trajectories while the dashed lines correspond to the depressed trajectories. The RV is intercepted when the trajectories intersect one another. These are the physical solutions that include gravity. Clearly, the physical trajectories are not straight line trajectories.
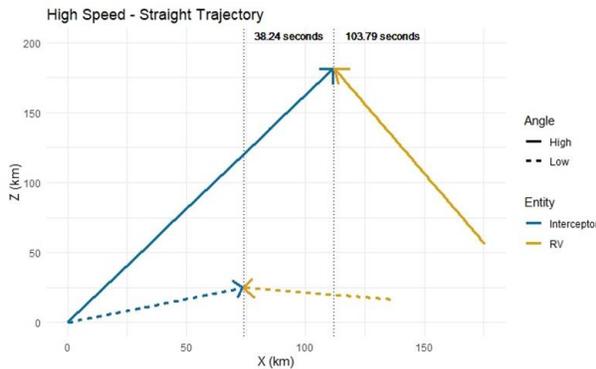

Figure 5: Feasible straight line intercept (without gravity) for high speed interceptor.
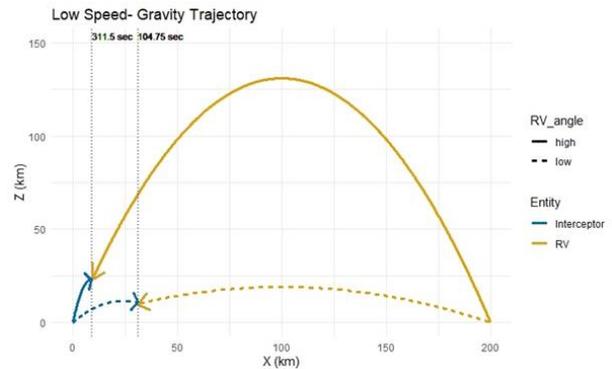
Figure 6: Feasible ballistic trajectory intercept (with gravity) for low speed interceptor.

Figure 7 shows the intercept of the RV trajectories in orange and the interceptor trajectories in blue (green) for an interceptor launch delay of 110 (50) seconds without gravity. The RV moves from right to left while the interceptor moves from left to right. The RV is intercepted when the trajectories intersect one another. These are the straight line solutions. Figure 8 shows the physical intercept of the RV trajectories in orange and the interceptor trajectories in blue (green) for an interceptor launch delay of 110 (50) seconds with gravity. The RV moves from right to left and the interceptor moves from left to right. The RV is intercepted when the trajectories intersect one another. These are the physical solutions that include gravity.

Figure 7 and Figure 8 illustrate the anomaly. That is, launching an interceptor later (110 sec as opposed to 50 secs) yield an earlier intercept (254 secs as opposed to 312 secs).
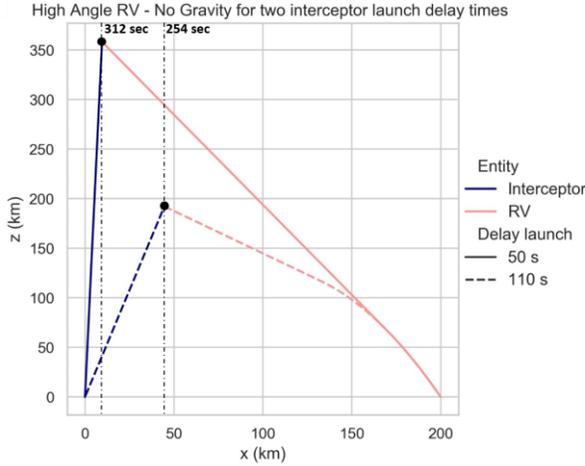

Figure 7: Feasible straight line intercept for two interceptor launch delay times without gravity after interceptor launching. Interceptor speed is MACH 4 from left to right and RV speed is MACH 5 from right to left.
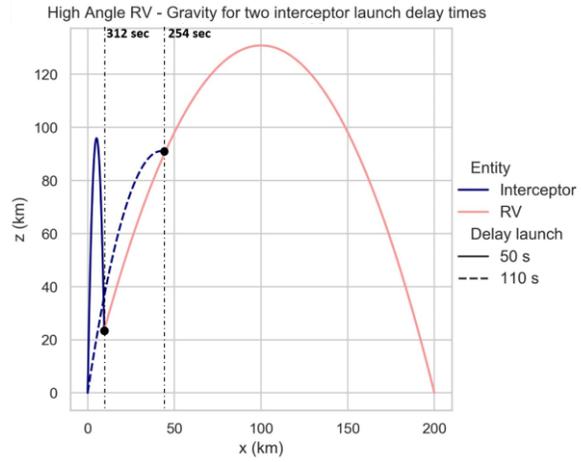
Figure 8: Feasible ballistic trajectory intercept for two interceptor launch delay times with gravity. Interceptor speed is MACH 4 from left to right and RV speed is MACH 5 from right to left.

4 THE ANOMALY IN THE INTERCEPT TIME

To show the anomaly i.e. there is a minimal intercept time T as a function of the interceptor launch delay time t, we provide an argument substantiating the fact that t_{int} is a decreasing function of t. While there are rigorous ways to show this, we make use of the Taylor series of t_{int} around the time of flight of the RV. This is feasible as the RV aims for the defense location that coincides with the interceptor launch location. This means that if the interceptor does not move or equivalently is delayed by the time of flight of the RV, the RV will reach the interceptor which implies that this is a solution in $t_{int} = 0$. Therefore, this is a feasible solution. We rewrite t_{int} as:

$$t_{int} = \frac{\Delta r^0}{v} \cdot \frac{-F + \sqrt{F^2 + (1 - \beta^2) \cdot (1 - \alpha^2)}}{1 - \beta^2} \cdot \frac{F + \sqrt{F^2 + (1 - \beta^2) \cdot (1 - \alpha^2)}}{F + \sqrt{F^2 + (1 - \beta^2) \cdot (1 - \alpha^2)}},$$

$$t_{int} = \frac{\Delta r^0}{v} \cdot \frac{(1-\alpha^2)}{F+\sqrt{F^2+(1-\beta^2)\cdot(1-\alpha^2)}} . \tag{2}$$

Since the detonation range is small, we neglect α in the proof of the anomaly. However, we include α in the final calculation. Let T_F be the time of flight of the RV, $\chi = t/T_F$ be the interceptor launch delay time scaled by T_F, R is the ground range from the RV launch site to the interceptor launch site, θ is the launch angle of the RV with respect to the ground, $\tan(\theta) = u_y/u_x$, and $\gamma = v^2 \cdot T_F^2/R^2$. The following parameters can be expressed as:

$$\left(\Delta r^0(t)\right)^2 = R^2 \cdot (1 - \chi)^2 \cdot (1 + tan(\theta)^2 \cdot \chi^2),$$

$$u(t)^2 = \frac{R^2}{T_F^2} \cdot [1 + tan(\theta)^2 \cdot (1 - 2 \cdot \chi)^2],$$

$$\vec{u}(t) \cdot \Delta \vec{r}^0(t) = \frac{R^2}{T_F} \cdot (1 - \chi) \cdot (1 - tan(\theta)^2 \cdot \chi + 2 \cdot tan(\theta)^2 \cdot \chi^2),$$

$$t_{int} = \frac{T_F \cdot (1 - \chi) \cdot (1 + tan(\theta)^2 \cdot \chi^2)}{(1 - tan(\theta)^2 \cdot \chi + 2 \cdot tan(\theta)^2 \cdot \chi^2) + \sqrt{\gamma + tan(\theta)^2 \cdot [-1 + 2 \cdot \chi + \chi^2 \cdot (\gamma - 1)]}},$$

$$t_{int} = T_F \cdot (1 - \chi) \cdot \bar{t}_{int},$$

$$\bar{t}_{int} = \frac{(1 + tan(\theta)^2 \cdot \chi^2)}{(1 - tan(\theta)^2 \cdot \chi + 2 \cdot tan(\theta)^2 \cdot \chi^2) + \sqrt{\gamma + tan(\theta)^2 \cdot [-1 + 2 \cdot \chi + \chi^2 \cdot (\gamma - 1)]}}. \tag{3}$$

Since $1 - \chi$ is a decreasing function in χ, if $\bar{t}_{int}$ is also decreasing in χ then t_{int} is decreasing in χ. We will show this below. Using Mathematica, we expand $\bar{t}_{int}$ about one in a Taylor series up to the second order in $1 - \chi$.

$$\bar{t}_{int} = \bar{t}_0 + \bar{t}_1 \cdot (1 - \chi) + \bar{t}_2 \cdot (1 - \chi)^2 + O((1 - \chi)^3),$$

$$\bar{t}_0 = \frac{a^2}{a^2 + a\sqrt{\gamma}},$$

$$\bar{t}_1 = \frac{(a^2 - 1) \cdot (a^2 - a\sqrt{\gamma})}{(a^2 + a\sqrt{\gamma})^2},$$

$$\bar{t}_2 = \frac{(a^2 - 1) \cdot \left[-5 \cdot a^2 \cdot \gamma + 4 \cdot a^4 \cdot \gamma + \gamma^2 + a^3 \cdot \sqrt{\gamma} + 3 \cdot a \cdot \gamma^{3/2} - 4 \cdot a^3 \cdot (\gamma)^{3/2} \right]}{2 \cdot \gamma \cdot (a + \sqrt{a \cdot \gamma})^3},$$

$$\bar{t}_2 = \frac{(a^2 - 1) \cdot (a - \sqrt{\gamma}) \cdot \sqrt{\gamma} \cdot (a^2 + 4 \cdot a \cdot \sqrt{\gamma} \cdot (a^2 - 1) - \gamma)}{2 \cdot \gamma \cdot (a + \sqrt{a \cdot \gamma})^3}, \tag{4}$$

where $a^2 = 1 + tan(\theta)^2 > 1$. As suggested in Figure 4, we consider $\gamma = v^2 \cdot T_F^2 / R^2 < 1$ meaning that the interceptor speed is less than the RV speed along the horizontal axis. Since the interceptor speed has to be greater than zero for the interceptor to travel, we also get $\gamma > 0$. Hence, $0 < \gamma < 1$. This implies that $\bar{t}_0 > 0$ and $\bar{t}_1 > 0$. Also $\bar{t}_2 > 0$ under a condition shown below. Let $\gamma = \lambda^2$, then the last factor in the numerator of $\bar{t}_2$ can be written as:

$$a^2 + 4 \cdot a \cdot \lambda \cdot (a^2 - 1) - \lambda^2. \tag{5}$$

which is a parabola in λ that opens down. There are two roots:

$$\lambda_- = 2 \cdot a \cdot (a^2 - 1) - \sqrt{\left(2 \cdot a \cdot (a^2 - 1) \right)^2 + a^2},$$

$$\lambda_+ = 2 \cdot a \cdot (a^2 - 1) + \sqrt{\left(2 \cdot a \cdot (a^2 - 1) \right)^2 + a^2}$$

as dictated by the quadratic equation. Since $a > 1$, $\lambda_- < 0$ and $\lambda_+ > 1$, therefore if $0 < \lambda^2 < 1$, Equation (5) is greater than or equal to zero. This confirms that $\bar{t}_2 > 0$. Assuming the Taylor series converges, we have a decreasing function $\bar{t}_{int}$.

To find the minimum, we solve the following equation numerically:

$$T' = 0 = [1 + t_{int}(t)'].$$

We choose Mathcad (Parametric Technology Corporation 2007) but other software such as Mathematica (Wolfram Research 2020) or algorithms such as the bisection algorithm could be used. We provide an example below. $R = 200\ km$, trajectory is lofted (high angle), $u = MACH\ 5$, and $v = MACH\ 4$. That is, the RV is initially 200 km away from the defense, the RV speed is $MACH\ 5$ and the interceptor speed is $MACH\ 4$. The intercept time T has a minimum when the interceptor launch delay time is equal to $t = 110.245\ sec$ (110.25 $secs$) if the detonation range is 5 m (0 m). This is consistent with the red circle on the yellow curve in Figure 4. As shown in Figure 2, depressed trajectories do not exhibit minima.

For completeness, below is the equation of motion for short range ballistic missiles (both the RV and the interceptor):

$$\vec{r}(t) = \begin{pmatrix} x \\ y \\ z \end{pmatrix} = \vec{r}_0 + \vec{v} \cdot t - \frac{1}{2} \cdot g \cdot t^2 \cdot \hat{z} ,$$

where $\vec{r}_0$ is the initial location of the ballistic vehicle; $\vec{v}$ is the initial velocity; t is the time measured from the moment the vehicle as at $\vec{r}_0$; g is gravity and $\hat{z}$ is the unit vector along the altitude from the ground. The vehicle can be launched from anywhere including from an aircraft for example (Burk and Foote 2009). This equation of motion is suitable for high level studies and does not include environmental effects such as air drags (de Carpentier 2014).

5   DISCUSSION

In this paper, we analyze a formula for intercept time of a ballistic RV by a ballistic interceptor at a non – zero detonation range. We show that there is an anomaly in the intercept time in the sense that launching the interceptor early does not necessarily yield an early intercept. Since the intercept time affects the number of engagement opportunities, the anomaly has ramifications in the probability of raid negation (the probability of neutralizing all RVs). By minimizing the intercept time, we may maximize the number of engagement opportunities: an idea that we will explore in the future. There are also many sensitivity analyses that can be done using the intercept time such as examining the ratio of the detonation range to the initial distance or the ratio of the RV's speed to the interceptor's speed etc. We endeavor to also undertake these analyses in the future.

REFERENCES

Amyot-Bourgeois, M., L. Serré, and P. Dobias. 2021. "Use of Agent-Based Modeling and Data Farming for the Army ISR Capability Assessment". In *Proceedings of 14th NATO 2020 OR&A Conference* MP-SAS-OCS-ORA-2020-EDT-03, STO Publisher.

Amyot-Bourgeois, M., G. Nikolakakos, and L. Serré. Forthcoming. "Investigation of GBAD system options using simulation and Data Farming". *Canadian Army Journal*. Forthcoming.

Armstrong, Michael J. 2014. "Modeling short-range ballistic missile defense and Israel's Iron Dome system". *INFORMS* 62(5):1028 – 1039.

Ballistic missile defenses. 2021. Carnegie endowment for international peace reports, 73 – 78.

Bate, Roger R., D. D. Mueller, and J. E. White. 1971. *Fundamentals of astrodynamics*. New York : Dover Publications.

Bourn, S. 2012. "Probabilistic shoot–look–shoot combat models". PhD thesis, School of Mathematical Sciences, The University of Adelaide, Adelaide, Australia.

Buontempo, J. T. 2015. "A trajectory for homeland ballistic missile defense". *Defense & Security Analysis* 31(2):99 – 109.

Burk, R., and B. Foote. 2009. "A preliminary analysis of loitering aircraft as a capability added to theater – level anti – ballistic missile systems". *Military Operations Research* 14:5–18.

Carpentier, G. J. P. de. 2014. "Analytical ballistic trajectories with approximately linear drag". *International Journal of Computer Games Technology* 2014(1):1.

Castle, C. J. E. and A. T. Crooks. 2006. "Principles and concepts of agent – based modelling for developing geospatial simulations". Centre for Advanced Spatial Analysis – London University College.

Cranford, K.. "Battle Area Region Threatened Model (BART)". NORAD – USNORTHCOM/AN (North American Aerospace Defense Command – United States Northern Command/Center for Aerospace Analysis), version 5.3.4x, accessed 12th January 2022.

Diallo, S. Y., C. J. Lynch, R. Gore, and J. J. Padilla. 2015. "Emergent behavior identification within an agent – based model of the ballistic missile defense system using statistical debugging". *Journal of Defense Modeling and Simulation* 13(3):275 – 289.

Lauren, M. K., and R. T. Stephen. 2002. "Map-Aware Non-uniform Automata (MANA) — A New Zealand approach to scenario modelling". *Journal of Battlefield Technology* 5(1):27-31.

Menq, J., Pan – chio Tuan, and Ta – Sheng Liu. 2007. "Discrete Markov ballistic missile defense system modeling". *European Journal of Operational Research* 178(2):560-578.

Mury, B. and B. Nguyen. 2007. "A recursive engagement simulation tree (REST) for use in maritime defense". Defense R&D Canada Atlantic Technical Memorandum TM 2006–096.

Nguyen, B., M. Amyot-Bourgeois, and B. Astles. forthcoming. "Intercept times against short-range ballistic re-entry vehicles". working paper, March 2022.

Nguyen, B., and D. Nguyen. 1996. "Optimal intercept course of vessels to a non–zero range". *SIAM (Society for Industrial and Applied Mathematics) Review* 38(4):647–649.

Nguyen, B. U. 2014. "Assessment of a ballistic missile defense system". *Defense & Security Analysis* 30(1):4–6.

Nguyen, B., P. A. Smith, and D. Nguyen. 1997. "An engagement model to optimize defense against a multiple attack assuming perfect kill assessment". *Naval Research Logistics* 44(7):687-697.

Parametric Technology Corporation. 2007. Mathcad 14.0.

Patriot. https://en.wikipedia.org/wiki/MIM-104 Patriot, accessed 12th January 2022.

Scud missile. https://en.wikipedia.org/wiki/Scud missile, accessed 12th January 2022.

Serré, L., M. Amyot-bourgeois, and B. Astles. 2021. "Use of Shapley Additive Explanations in interpreting agent-based simulations of military operational scenarios", In *Proceedings of the 2021 Annual Modeling and Simulation Conference (ANNSIM'21)*. July 19th – 21st, Virtual, 1-12.

Soland, R. M. 1987. "Optimal terminal defense tactics when several sequential engagements are possible". *Operations Research* 35(4):537–542.

Vallado, D. A. 1997. "Fundamentals of astrodynamics and applications", *McGraw – Hill Primis Custom Pub.* Howthorne, CA, USA.

Weitz, R. 2013. "US missile defense: closing the gap". *World Affairs* 176(2):80-87.

Wilkening, D. A. 1999. "A simple model for calculating ballistic missile defense effectiveness". *Science & Global Security* 8(2):183–215.

Wolfram Research, Inc. 2020. Mathematica, Version 12.2, Champaign, IL.

AUTHOR BIOGRAPHIES

P. BAO U. NGUYEN is an Adjunct Professor in mathematics at the University of Ottawa as well as a Senior Defence Scientist at Defence R&D Canada – Centre for Operational Research and Analysis. He earned his Ph.D. in theoretical particle physics from McGill University. Professor Nguyen has received many awards including the Koopman Prize for the outstanding paper in military decision analysis. He is an avid soccer and badminton player. His email address is p.bao.u.nguyen@gmail.com.

MAUDE AMYOT-BOURGEOIS is a Junior Defence Scientist with Defence Research and Development Canada's Centre for Operational Research and Analysis. Since 2019, she has worked in collaboration with her colleagues from the Canadian Army Operational Research and Analysis Team on various combat simulation and NATO wargaming studies. She obtained her Master's degree in physics from the University of Ottawa, Canada. Her email address is maude.amyot-bourgeois@ecn.forces.gc.ca.

BRITTANY C. ASTLES is a Junior Defence Scientist with Defence Research and Development Canada's Centre for Operational Research and Analysis. Since 2021 she has worked primarily on data assessment for simulations projects, and NATO wargames. As well as studying the use of machine learning on terrorist attacks cassualty rates based on historical data. She received her Master of Science degree in geography with a specialty in data science from Carleton University in Ottawa. Her email address is brittany.astles@ecn.forces.gc.ca.